Restricted Rotation and NOE Transfer: A Conformational Study of Some Substituted (9-Anthryl)carbinol Derivatives

Innocenzo de Riggi, Albert Virgili,* Maria de Moragas, and Carlos Jaime

Departament de Química, Universitat Autònoma de Barcelona, 08193 Bellaterra, Spain

Received June 20, 1994[⊗]

Four alkyl- and aryl(9-anthryl)carbinols (methyl, isopropyl, *tert*-butyl, and phenyl) were synthesized and revealed restricted rotation about the C_9-C_{11} bond. Their free energy of activation for rotation has been determined, being 11.0, 14.0, 21.7, and 9.8 kcal/mol, respectively. The application of NOE enhancement and relaxation time measurements for the determination of the activation energy for bond rotation is described. The good agreement with the values obtained with the coalescence temperature method bears out that the NOE based approach is a good alternative for the determination of high rotational barriers. Molecular Mechanics (MM2) calculations give values close to the experimental ones.

Introduction

The energy associated with a kinetic process such as the rotation around a σ bond can be measured by dynamic NMR spectroscopy. The most common method is the well-known line shape analysis[1] of two absorptions via the determination of their coalescence temperature or via simulation of the exchange broadened resonances. The coalescence-based technique is appropriate for the measurement of rotational activation energies within a range of 8–16 kcal·mol^{-1}. However, the time scale NMR spectroscopy is often too low for the coalescence point to be determined in higher energy processes. Working at higher temperatures rapidly becomes difficult, requiring specific experimental conditions and probes. The Hoffman–Forsèn double resonance method[2] can also be applied. Such difficulties associated with high activation energies can occur in the case of (9-anthryl)carbinol derivatives bearing a substituent in the α position to the hydroxyl group; for example, recent measurements[3] have shown that there is restricted rotation around the C_9-C_{11} bond of the (*R*)-(−)-2,2,2-trifluoro-1-(9-anthryl)ethanol (**3**) (see Figure 1) and that the activation energy is 14.5 kcal·mol^{-1}. Replacing the trifluoromethyl group by a much larger substituent increases the steric hindrance and will probably result in rotational energy barriers much higher than 16 kcal·mol^{-1}.

In this paper we describe an alternative method for measuring these high energy barriers; our method is based upon the observation of NOE enhancements and overcomes the difficulties which existing methods have with such high energy processes.

Theory

Solomon's[4] equation describing NOE can be modified[5] to include the effects of conformational equilibrium due to the rotation about a bond.

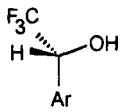

Figure 1. Aryl (*R*)-(−)-2,2,2-trifluoroethanol derivatives: **1**, Ar = phenyl; **2**, Ar = α-naphthyl; **3**, Ar = 9-anthryl.

Scheme 1. Two-Spin System with Two-Site Exchange

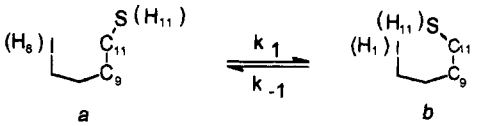

Our model assumes the exchange equilibrium (Scheme 1) between two forms, a and b, with forward and backward rate constants k_1 and k_{-1}.

In Scheme 1 a and b are the two conformers of (9-anthryl)carbinol derivatives. Due to C_2 symmetry the rate constants are equal and will be set to k. Solomon's equation for a two-spin system with two-site exchange can be expressed as

$$\frac{dI_{1z}}{dt} = -R_{I_1}(I_{1z} - I^{\circ}_{1z}) - \sigma_{I_1S}(S_z - S^{\circ}_z) + k(I_{8z} - I^{\circ}_{8z}) - k(I_{1z} - I^{\circ}_{1z}) \quad (1)$$

$$\frac{dI_{8z}}{dt} = -R_{I_8}(I_{8z} - I^{\circ}_{8z}) - \sigma_{I_8S}(S_z - S^{\circ}_z) + k(I_{1z} - I^{\circ}_{1z}) - k(I_{8z} - I^{\circ}_{8z}) \quad (2)$$

where I_{1z} is the longitudinal magnetization of H_1 (the closest proton to H_{11}), S_{1z} is the longitudinal magnetization of the irradiated spin (H_{11}), and I_{8z} is the longitudinal magnetization of H_8; the exchange is between H_1 and H_8. The degree symbol indicates equilibrium magnetization. R_I is the longitudinal relaxation rate constant for spin I, and σ_{IS} the cross relaxation rate constant between I and S.

The variation in the magnetization of spin I caused by saturation of S is the result of various contributing factors. The first two terms are found in systems without exchange and are the longitudinal and cross relaxation rates. Two extra terms must be added because of the exchange. These represent the loss and the recovery of I magnetization brought by the rotation process.

[⊗] Abstract published in *Advance ACS Abstracts,* December 1, 1994.

(1) (a) Oki, M. In *Applications of Dynamic NMR Spectroscopy to Organic Chemistry*; VCH: Deerfield Beach, FL, 1985. (b) Sandström, J. In *Dynamic NMR Spectroscopy*; Academic Press: London, New York, 1982.

(2) (a) Hoffman, R. A.; Forsén, S. *Prog. NMR Spectrosc.* **1966**, *1*, 89. (b) Faller, J. W. In *Determination of Organic Structures by Physical Methods*; Academic Press: New York and London, 1973; Vol. 5.

(3) Jaime, C.; Virgili, A.; Claramunt, R. M.; López, C.; Elguero, J. *J. Org. Chem.* **1991**, *56*, 6521.

(4) Solomon, I. *Phys. Rev.* **1948**, *99*, 559.

0022-3263/95/1960-0027$09.00/0

As H_8 is much more distant from H_{11} (the irradiation proton) than H_1, we assume that the cross-relaxation between H_8 and H_{11} can be ignored: $\sigma_{I8S} = 0$. Using the appropriate conditions for the steady state[5] ($S_z = 0$, $dI_z/dt = 0$), and taking I_{1z}° and I_{8z}° to be equal to S_z° as all are from the same nuclear species, eqs 1 and 2 can be rewritten as eqs 3 and 4:

$$\frac{dI_{1z}}{dt} = -R_{I_1}(I_{1z} - I_{1z}^\circ) + \sigma_{I_1S}S_z^\circ + k(I_{8z} - I_{8z}^\circ) - k(I_{1z} - I_{1z}^\circ) = 0 \quad (3)$$

$$\frac{dI_{8z}}{dt} = -R_{I_8}(I_{8z} - I_{8z}^\circ) + k(I_{1z} - I_{1z}^\circ) - k(I_{8z} - I_{8z}^\circ) = 0 \quad (4)$$

Dividing eqs 3 and 4 by I_{1z}°, I_{8z}°, or S_z°, as appropriate (all are equal), we obtain

$$-R_{I_1}\frac{(I_{1z} - I_{1z}^\circ)}{I_{1z}^\circ} + \sigma_{I_1S} + k\frac{(I_{8z} - I_{8z}^\circ)}{I_{8z}^\circ} - k\frac{(I_{1z} - I_{1z}^\circ)}{I_{1z}^\circ} = 0 \quad (5)$$

$$-R_{I_8}\frac{(I_{8z} - I_{8z}^\circ)}{I_{8z}^\circ} + k\frac{(I_{1z} - I_{1z}^\circ)}{I_{1z}^\circ} - k\frac{(I_{8z} - I_{8z}^\circ)}{I_{8z}^\circ} = 0 \quad (6)$$

If $f_I(S)$ is the NOE enhancement of spin I resulting from the saturation of spin S, then eqs 5 and 6 become

$$f_{I_1}(S) = \frac{\sigma_{I_1S}}{(R_{I_1} + k)} + \frac{k}{(R_{I_1} + k)}f_{I_8}(S) \quad (7)$$

$$f_{I_8}(S) = \frac{k}{(R_{I_8} + k)}f_{I_1}(S) \quad (8)$$

These equations are a special case of the more general situation for the NOE in a system with two-site exchange.[5]

Equation 7 shows that enhancement of I_1 is the sum of two contributions: The normal NOE due to cross-relaxation between I_1 and S and the enhancement transferred from I_8 to I_1 via the exchange process. Equation 8 shows that the enhancement on I_8 is due only to the enhancement of I_1 being transferred from I_8 by the exchange process; there is no direct NOE enhancement on I_8 caused by saturation of S.

Finally, a relationship between the NOE enhancement of H_8 and the difference between the NOE enhancements of H_1 and H_8 can be deduced from eq 8:

$$\frac{f_{I_8}(S)}{(f_{I_1}(S) - f_{I_8}(S))} = \frac{k}{R_{I_8}} \quad (9)$$

If, at one temperature, the NOE enhancements of both protons H_1 and H_8 and the relaxation rate of H_8 are measured, the rate constant for the exchange process can be deduced. The free energy of activation for the rotation can then be determined using Eyring's equation ($\Delta G^\ddagger = (4.576 \times 10^{-3})T(10.319 + \log(T/k))$).

Application to Some Substituted (9-Anthryl)-carbinol Derivatives. Enantiomerically pure (+)- and (−)-aryl-2,2,2-trifluoroethanols **1**−**3** (Figure 1), also known as Pirkle's alcohols, are widely used as optically active NMR reagents.[6] The 9-anthryl derivative, **3**, shows the greatest nonequivalences between enantiomeric solutes owing to an increased anisotropic effect with respect to naphthyl and phenyl derivatives.[7]

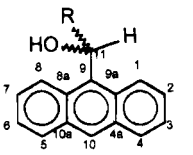

Figure 2. Alkyl and aryl derivatives of (9-anthryl)carbinol: **4**, R = Me; **5**, R = Ph; **6**, R = i-Pr; **7**, R = t-Bu.

A detailed description of the NMR properties of the (*R*)-(−)-trifluoro alcohol **3** and an attempt to correlate these with its behavior as a chiral agent have been completed in our laboratory.[3] The free energy of activation for the rotation about the C_9-C_{11} bond was evaluated and proved to be in quite good agreement with the value calculated by molecular mechanics (MM2)[8,9] (see Table 1). Unresolved halo derivatives of (9-anthryl)carbinol have been already studied by Ottinger[10] and co-workers who found similar values for the energies of activation.

This study has been extended to a series of four alkyl- and aryl(9-anthryl)carbinol derivatives **4**−**7** (see Figure 2), and free energies of activation for the C_9-C_{11} bond rotations have been determined. The conformational exchange rate for the new compound **7** is considerably lower than for the others, owing to severe steric interactions between the *tert*-butyl group and the anthracenic *peri* protons.

The rotational barrier around the C_9-C_{11} bond of alcohols **4**−**6** has been measured by determining the temperature at which the resonances from the anthracenic *peri* protons H_1 and H_8 coalesce (see Table 1). Unfortunately, this was not possible for **7** as the coalescence temperature could not be reached (this temperature was calculated using subsequent data to be about 470 K). The analysis by simulation of the exchange broadened resonances was no longer possible because at the highest accessible temperature, 380 K, no appreciable broadening of corresponding signals was observed.

For compounds **6** (see Table 2) and **7** (see Table 3), NOE difference experiments were performed by saturation of proton H_{11}, for a range of temperatures at which the signals of the *peri* protons were distinct. Different enhancements of H_1 and H_8 were observed. The rate constant k and the free energy of activation for the C_9-C_{11} bond rotation were determined by the method described above.

(5) Neuhaus, D.; Williamson, M. In *The Nuclear Overhauser Effect in Structural and Conformational Analysis*; VCH: New York, 1989.

(6) (a) Pirkle, W.; Hoekstra, M. S. *J. Org. Chem.* **1974**, *39*, 3904. (b) Pirkle, W. H.; Hauske, J. R. *J. Org. Chem.* **1976**, *41*, 801. (c) Pirkle, W. H.; Sikkenga, D. L.; Paulin, M. S. *J. Org. Chem.* **1977**, *42*, 384. (d) Pirkle, W. H.; Rinaldi, P. L. *J. Org. Chem.* **1977**, *42*, 3217. (e) Pirkle, W. H.; Simmons, K. A. *J. Org. Chem.* **1981**, *46*, 3239. (f) Pirkle, W. H.; Hoover, D. J. *Top. Stereochem.* **1982**, *13*, 263. (g) Lipkowitz, K. B.; Demeter, D. A.; Parish, C. A. *Anal. Chem.* **1987**, *59*, 1733.

(7) (a) Pirkle, W. H.; Sikkenga, D. L. *J. Org. Chem.* **1977**, *42*, 1370. (b) Pirkle, W. H.; Boeder, Ch. W. *J. Org. Chem.* **1977**, *42*, 3697. (c) Casarini, D.; Davalli, S.; Lunazzi, L.; Macciantelli, D. *J. Org. Chem.* **1989**, *54*, 4616. (d) Foces-Foces, C.; Hernández Cano, F.; Martinez-Ripoll, M.; Faure, R.; Roussel, C.; Claramunt, R. M.; López, C.; Sanz, D.; Elguero, J. *Tetrahedron Asymmetry* **1990**, *1*, 65.

(8) Osawa, E.; Jaime, C.; Fujiyoshi, T.; Goto, H.; Imai, K. *JCPE Newsletter* **1989**, *1*, program no. 9 (VAX version).

(9) (a) Allinger, N. L.; Yuh, N. Y. *QCPE* **1980**, *12*, 395. (b) Allinger, N. L. *J. Am. Chem. Soc.* **1977**, *99*, 8127.

(10) Ben Hassine, B.; Gorsane, M.; Pecher, J.; Martin, R. H.; Defay, N.; Ottinger, R. *Bull. Soc. Chim. Belg.* **1985**, *94*, 425.

Table 1. Data from Observation of Coalescence Temperatures and MM2 Calculations

R	T_c (K)	$\delta\nu_{max}$ (Hz)	$\Delta G^{\ddagger a}$ at T_c (kcal·mol^{-1})	$\Delta H_f^{\ddagger b}$ (MM2) (kcal·mol^{-1})
Ph:5	202	40 at 188 K	9.8	7.95
Me:4	245	356 at 210 K	11.0	10.92
iPr:6	306	290 at 260 K	14.0	14.30
CF_3:3[c]	320	373 at 245 K	14.5	15.20
tBu:7		380 at 242 K		21.80

[a] The error on $\Delta G^{\ddagger}$ calculated from the coalescence temperature has been evaluated to ±0.1 kcal·mol^{-1}. T_c is the coalescence temperature and $\Delta\nu_{max}$ the maximum shift difference between H_1 and H_8 at the indicated temperature. [b] $\Delta H_f^{\ddagger}$ is the difference between the enthalpies of formation of the ground-state and the transition-state rotamers at 25 °C. Assuming entropy only varies by a small amount between one rotamer and another, this quantity can be compared directly with the experimental values of free energy of activation. [c] Cf. ref 2.

Table 2. Relaxation Rate and NOE Measurements on Alcohol 6

T (K)	$f_{I1}(S)$ (%)	$f_{I8}(S)$ (%)	R_{I1} (s^{-1})	R_{I8} (s^{-1})	k (s^{-1})	$\Delta G^{\ddagger}$ (kcal·mol^{-1})
210	26	2	2.100	1.284	0.107	13.1
215	25	3.5	1.825	1.195	0.195	13.1
220	23	5.5	1.650	1.083	0.340	13.2
225	21	9.5	1.506	1.034	0.854	13.1
230	19.5	12	1.307	0.990	1.584	13.1
235	18.5	14	1.136	0.936	2.912	13.2
240	18	16	0.977	0.900	7.200	13.0
245	17.5	17	0.845	0.845	28.730	12.6

Table 3. Relaxation Rate and NOE Measurements on Alcohol 7

T (K)	$f_{I1}(S)$ (%)	$f_{I8}(S)$ (%)	R_{I1} (s^{-1})	R_{I8} (s^{-1})	k (s^{-1})	$\Delta G^{\ddagger}$ (kcal·mol^{-1})
320	24.0	0.5	0.385	0.204	0.0043	22.2
330	20.5	3.5	0.322	0.187	0.0385	21.5
340	19.5	6.0	0.267	0.171	0.0760	21.7
350	15.0	7.5	0.231	0.170	0.1700	21.8
360	13.0	9.5	0.194	0.169	0.4587	21.8
370	11.5	10.0	0.180	0.168	1.1200	21.7
380	10.5	10.5	0.167	0.167		

Molecular Mechanics Treatment. The conformational exchange processes were reproduced by driving both the $\omega_1 = C_{9a}-C_9-C_{11}-C_{12}$ and $\omega_3 = C_9-C_{11}-O-H$ dihedral angles for **4** and **7** or ω_1 together with $\omega_2 = C_9-C_{11}-C_{12}-C_{13}$ (see Figure 3) for compounds **5** and **6** (for these two last compounds, the optimization of ground-state conformations was carried out by a further driving of ω_3 using the option TREE within the MM2PRIME program).[8] All these angles were rotated from −180° to 180°, at 15° steps, except for the phenyl derivative for which ω_2 was rotated only from 0° to 180° (owing to the C_2 symmetry of the phenyl group). The lower energy pathways between ground-state and transition-state conformations were determined from the obtained torsional energy surfaces (Figure 4).

Results and Discussion

The free energy of activation was calculated using the modified Eyring's equation ($\Delta G^{\ddagger} = (4.576 \times 10^{-3})T_c(9.972 + \log(T_c/\delta\nu))$) at the coalescence temperature. For compound **5**, coalescence could also be measured from the proton pair (H_4, H_5). As can be seen from Table 1, rotation in **5** is easier than in **4**, this is because the phenyl group can rotate to minimize steric interactions with the *peri* protons of the anthracene, while the symmetrical methyl group cannot. Compound **6** exhibits a rotational

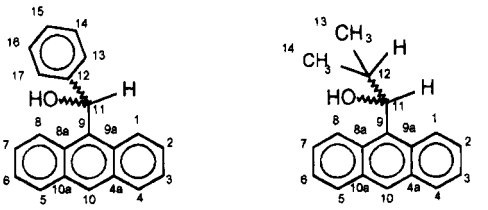

Figure 3. Numbering of the carbons in compounds **5** and **6**.

activation energy similar to that of the trifluoro derivative. Owing to its high barrier of rotation, the homochiral *tert*-butyl derivative **7** (or some derivative of it) as a chiral solvating agent could be of particular interest. The results compiled in Tables 2 and 3 show that the NOE enhancements observed on proton H_8 are due to the exchange between H_1 and H_8 caused by rotation about the C_9-C_{11} bond. Indeed, at 210 K for **6** and 320 K for **7**, the internal rotation is so slow that there is almost no NOE enhancement of proton H_8. At sufficiently high temperature the exchange process between H_1 and H_8 becomes faster than the relaxation rates, $k \gg T_1^{-1}$, and as a result the NOE enhancements and longitudinal relaxation rates are averaged (this is the case at 245 K for **6** and at 380 K for **7**). However, in this range of temperatures, the exchange is still slow enough on the chemical shift time scale, $k \ll \Delta\delta$, that H_1 and H_8 give rise to separated signals. It is for such processes that the method using NOE measurement is highly suited.

The accuracy of the determined values of k and $\Delta G^{\ddagger}$ is clearly dependent on the method used. The precision on the rate constants determined by eq 9 is at its worst when small NOE enhancements are measured (as on H_8 at the lowest temperatures) and when the NOE enhancements on H_1 and H_8 are averaged (as the determination of k depends on the difference between these NOE enhancements). The resulting values of free energy of activation have an error of $<\pm 0.3$ kcal/mol, owing to the logarithmic relationship between $\Delta G^{\#}$ and k.

The value of the activation energy, calculated by the NOE method (12.6−13.2 kcal·mol^{-1}, Table 2), for the (9-anthryl)isopropylcarbinol (**6**), is in good agreement with that encountered by observation of the coalescence temperature (14 kcal·mol^{-1}, Table 1). In all cases, the results of MM2 calculations reproduce the experimental values quite well.

Tables 4−7 contain the complete assigned ^{1}H NMR spectra of compounds **4**−**7**. The first three compounds have been described at two temperatures: at a "high" temperature where the molecules appear symmetrical, i.e., only one signal for each of the following pairs (H_1, H_8), (H_2, H_7), (H_3, H_6), (H_4, H_5) is observed, and at a "low" temperature where each proton gives a separate resonance. These spectra were simulated,[11] whenever it was possible, to make complete assignments. In this way, all the chemical shifts were assigned and all the coupling constants in some complex spin systems were determined.

The protons assignments for compounds **5** and **7** have been confirmed at each temperature by homonuclear COSY and NOE difference experiments. The ordering of the chemical shift of the sequence H_2, H_3, H_6, H_7 for **6** at 210 K was supposed to be the same as in **7** ($\delta H_2 > \delta H_3 > \delta H_6 > \delta H_7$).

(11) Simulations have been achieved using version 930501 of the Bruker "WIN-DAISY" program.

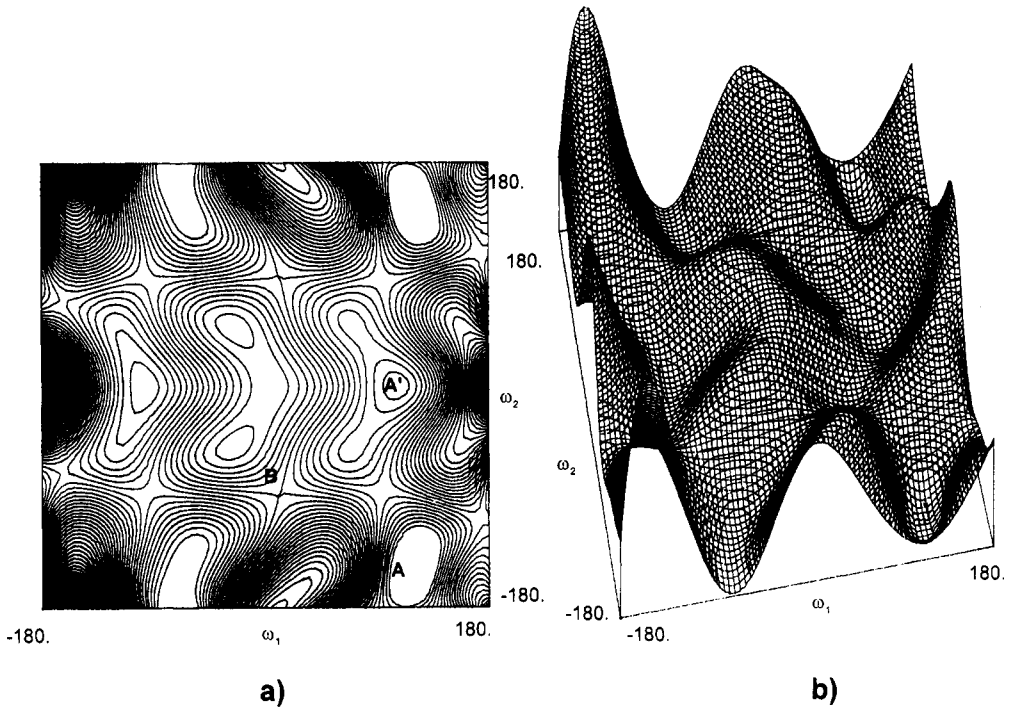

Figure 4. View of the torsional energy surface relative to compound **5**. Contour lines were drawn each 1 kcal·mol^{-1}: (a) contour map, (b) three dimensional.

Table 4. ^{1}H NMR Chemical Shifts (δ in ppm versus TMS) and Coupling Constants (J in Hz) of Compound 4 in C_3D_6O

^{1}H	297 K	200 K	J (Hz) (297 K)
H_1	8.82 (d[a])	8.40 (d[a])	$J_{1,2} = 9.1$; $J_{1,3} = 1.1$; $J_{1,4} = 0.8$
H_8	8.82 (d[a])	9.28 (m[a])	$J_{8,10} = 0.9$
H_2	7.47 (m)[b]	7.43–7.58[a]	$J_{2,3} = 6.4$; $J_{2,4} = 1.5$
H_7	7.47 (m)[b]		$J_{7,8} = 9.1$
H_3	7.46 (m)[b]		$J_{3,4} = 8.5$
H_6	7.46 (m)[b]		$J_{6,8} = 1.1$
H_4	8.04 (m)	8.03–8.13	$J_{4,10} = -0.8$
H_5	8.04 (m)	(m[a])	$J_{5,6} = 8.5$; $J_{5,7} = 1.5$; $J_{5,8} = 0.8$; $J_{5,10} = -0.8$
H_{10}	8.45 (s)	8.53 (s)	
H_{11}	6.48 (qd)	6.47 (qd)	$J(H_{11},Me) = 6.8$; $J(H_{11},OH) = 3.4$
OH	4.66 (dq)	5.24 (d)	$J(OH,Me) = 0.4$
Me	1.82 (dd)	1.75 (d)	

[a] Broad signal. [b] These signals can be reversed.

Table 5. ^{1}H NMR Chemical Shifts (δ in ppm versus TMS) and Coupling Constants (J in Hz) of Compound 5 in C_3D_6O

^{1}H	298 K	188 K	J (Hz) (188 K)
H_1	8.57 (d[b])	8.55 (d[a])	$J_{1,2} = 8.9$; $J_{1,3} = 1.5$; $J_{1,4} = J_{1,10} = 0.6$
H_8	8.57 (d[b])	8.65 (d[a,b])	$J_{8,10} = 0.8$
H_2	7.41 (m)	7.30 (dd[a,b])	$J_{2,4} = 1.5$; $J_{2,3} = 6.8$
H_7	7.41 (m)	7.63 (dd[a,b])	$J_{7,8} = 9.2$
H_3	7.45 (m)	7.40 (dd[a,b])	$J_{3,4} = 8.5$
H_6	7.45 (m)	7.58 (dd[a,b])	$J_{6,7} = 6.3$; $J_{6,8} = 1.7$
H_4	8.07 (dm)	8.07 (d)	$J_{4,10} = -0.6$
H_5	8.07 (dm)	8.19 (d)	$J_{5,6} = 8.4$; $J_{5,7} = 1.7$; $J_{5,8} = 0.9$; $J_{5,10} = -0.9$
H_{10}	8.56 (s[b])	8.64 (s[b])	
H_{11}	7.44 (d[b])	7.42 (d[b])	$J(H_{11},OH) = 4.0$
OH	5.44 (d)	6.07 (d)	
$H_{13} = H_{17}$	7.36 (m)	7.30 (d[b])	$J_{13,14} = 7.5$; $J_{13,15} = 1.5$; $J_{13,16} = 0.8$; $J_{13,17} = 1.8$
$H_{14} = H_{16}$	7.24 (tm)	7.27 (t[b])	$J_{14,15} = 7.5$; $J_{14,16} = 1.5$; $J_{14,17} = 0.8$; $J_{16,17} = 7.2$
H_{15}	7.16 (tm)	7.18 (t)	$J_{15,16} = 7.3$; $J_{15,17} = 1.5$

[a] Broad signal. [b] Superimposed signal.

MM2 Theoretical Calculations. The individual contributions of the low energy conformers (minima) which participate in the rotation process have been analyzed for each compound (Table 8). The population was obtained by Boltzmann's distribution at 25 °C. In all cases the ground-state conformation was reached when the R group was almost orthogonal to the anthracene (ω_1 is about ±100 °C in **4**, **6**, and **7** and 120 °C in **5**). For the methyl derivative **4**, the C_9-C_{11} bond rotation passes through an intermediate low energy conformer whose contribution is only 0.01%. In both the ground-state and the transition-state conformations of compounds **5** and **6** the R group rotates so as to minimize the steric interactions with the anthracenic *peri* protons; this is shown by the various values of the dihedral angle $\omega_2 = C_9-C_{11}-C_{12}-C_{13}$. Figure 4 clearly shows this for compound **5**. The conformational pathway, taken from the ground-state structure "A" during a 180° rotation about the C_9-C_{11} bond, requires first the change of the phenyl conformation from "A" to "A'", where the conformation of the hydroxyl group has also changed, and from there it goes through the transition state "B" down again to "A". In Figure 4, we can also notice large low energy regions around the ground-state conformation indicating that the rotation of the phenyl group is relatively free. In the case of alcohol **6**, a stable intermediate form (1.69 kcal·mol^{-1} above the absolute minimum and having a population of 5.17%) is involved before the energy falls again to that of the lowest energy rotamer. This stable intermediate form is not related to large changes in the hydroxyl group conformation (similar ω_3 values) but to different arrangements of the i-Pr and anthryl groups, as indicated by their ω_1 and ω_2 values (Table 8). The rotation process leads directly to the lowest minimum for the *tert*-butyl compound **7** as it does for the phenyl one **5**.

Experimental Section

Materials. Grignard reagents were purchased from Aldrich and used without further purification. Melting point is

Table 6. ^{1}H NMR Chemical Shifts (δ in ppm versus TMS) and Coupling Constants (J in Hz) of Compound 6 in C_3D_6O

^{1}H	324 K	210 K	J(Hz) (210 K)
H_1	8.80 ([a])	8.51 (d[c])	$J_{1,2}$ = 9.2; $J_{1,3}$ = 1.1; $J_{1,4}$ = 0.8; $J_{1,10}$ = 0.9
H_8	8.80 ([a])	9.15 (m)	$J_{8,10}$ = 0.9
H_2	7.45 (m[b])	7.51 (m)	$J_{2,3}$ = 6.4; $J_{2,4}$ = 1.4
H_7	7.45 (m[b])	7.47 (m)	$J_{7,8}$ = 8.8
H_3	7.44 (m[b])	7.48 (m)	$J_{3,4}$ = 8.6
H_6	7.44 (m[b])	7.48 (m)	$J_{6,7}$ = 6.5
H_4	8.03 (m)	8.08 (m)	$J_{4,10}$ = −0.6
H_5	8.03 (m)	8.07 (m)	$J_{5,6}$ = 8.5; $J_{5,7}$ = 1.4; $J_{5,8}$ = 0.7; $J_{5,10}$ = −0.6
H_{10}	8.44 (s)	8.53 (s[c])	
H_{11}	5.86 (dd)	5.82 (dd)	$J(H_{11},OH)$ = 3.5; $J_{11,12}$ = 10.1
OH	4.54 (d)	5.26 (d)	
Me_1	1.37 (d)	1.35 (d)	
Me_2	0.54 (d)	0.44 (d)	
H_{12}	2.72 (dspt)	2.67 (dspt)	$J(H_{12},Me_1)$ = 6.4; $J(H_{12},Me_2)$ = 6.9

[a] Broad Signal. [b] These signals can be reversed. [c] Superimposed signal; spt = septet.

Table 7. ^{1}H NMR Chemical Shifts (δ in ppm versus TMS) and Coupling Constants of Compound 7 in C_3D_6O

^{1}H	297 K	J (Hz)
H_1	8.47 (dm[a])	$J_{1,2}$ = 9.2; $J_{1,3}$ = 1.0; $J_{1,4}$ = 0.6; $J_{1,10}$ = 0.9
H_8	9.47 (dm)	$J_{8,10}$ = 0.9
H_2	7.48 (m)	$J_{2,4}$ = 1.4
H_7	7.38 (m)	$J_{7,8}$ = 9.2
H_3	7.44 (m)	$J_{3,4}$ = 8.5
H_6	7.42 (m)	$J_{6,7}$ = 6.6; $J_{6,8}$ = 1.1
H_4	8.04 (dm)	$J_{4,10}$ = −0.6
H_5	7.99 (dm)	$J_{5,6}$ = 8.6; $J_{5,7}$ = 1.5; $J_{5,8}$ = 0.8; $J_{5,10}$ = −0.6
H_{10}	8.47 (s[a])	
H_{11}	6.24 (d)	$J(H_{11},OH)$ = 4.4
OH	4.88 (d)	
Me	1.01 (s)	

[a] Superimposed signal.

uncorrected. Column chromatography was performed on silica gel 60 (SDS 2000027).

NMR Measurements. NMR spectra at variable temperatures were recorded using a Bruker AC400 WB spectrometer, with a 5-mm QNP probe and using CD_3COCD_3 as the solvent. The operating frequency was 400.16 MHz for ^{1}H.

The temperature of the probe was calibrated by the methanol standard method, and a delay of 600 s was used before recording the NMR spectra at each new temperature. All the NOE and inversion-recovery experiments were recorded using sealed sample tubes in which the dissolved oxygen had been first removed by the freeze−thaw technique (see Chapter 5 of ref 1). NOE difference spectra were obtained using 10 s of low-power (typically 55 L, 6.8 mW) presaturation; two dummy scans were used. The reproducibility was smaller than 1%. The resulting free induction decays containing 8 K data points were transformed to 16 K, points with zero filling. Relaxation times were measured by the inversion-recovery method using a 30 s relaxation delay.

Computational Details. Calculations were performed on a VAX-8820 computer at the Computer Center of the Universitat Autònoma de Barcelona, using the MM2PRIME program.[8] Allinger's[9] MM2(77) force field together with all MM2(85) parameters have been used throughout this work.

Preparation of the (9-Anthryl)-*tert*-butylcarbinol (7). Typical Procedure: A solution of 1 g (4.85 mmole) of 9-anthraldehyde in 30 mL of dry THF was placed in a 100 mL round-bottom flask closed with a septum and stirred at 0 °C under inert atmosphere. Then 2.9 mL (1.2 equiv) of a 2 M solution in THF of *tert*-butylmagnesium chloride were added dropwise during 30 min with a syringe. After the addition was complete, the solution was stirred at 0 °C for 1 h and 3 h at room temperature. The mixture was cooled at 0 °C and slowly hydrolyzed with 20 mL of a 10% aqueous solution of ammonium chloride. The organic layer was separated and the aqueous layer was extracted three times with 20 mL of diethyl ether. The organic layers were dried over magnesium sulfate and filtered. After evaporation of the solvent, the crude product was purified by liquid flash chromatography on silica gel with a 50:50 mixture of CH_2Cl_2/petroleum ether, affording after removal of the solvent 0.77 g (60% yield) of (9-anthryl)-*tert*-butylcarbinol as a fine powdered yellow solid. Further purification can be achieved by recrystallization in cyclohexane (mp 125−126 °C). Anal. Calcd for $C_{19}H_{20}O$): C, 86.32; H, 7.63. Found: C, 86.36; H, 7.73. MS: *m/z* (relative intensities) 265 (M^+ + 1, 3), 264 (M^+, 14), 208 (19), 207 (100), 179 (51), 178 (38).

Table 8. Relative Boltzmann Distribution (T) of the Low Energy Conformers without Considering Entropy Contributions and Dihedral Angles[a]

	ΔH_f	%	ω_1	ω_2[b]	ω_3
4	0.00	97.80	100.8		−3.4
	2.43	1.10	98.6		141.9
	2.44	1.09	−76.7		75.1
	5.02	0.01	161.1		38.9
4‡	10.9		40.0		−20.0
5	0.00	90.94	121.3	−40.0	−63.8
	1.47	7.55	121.7	−38.1	178.7
	2.47	1.41	121.9	−39.0	52.7
	4.02	0.10	−97.3	34.6	152.1
5‡	7.95		0.1	75.0	−91.1
6	0.00	89.45	103.8	−179.9	−4.5
	1.69	5.17	85.1	64.3	13.1
	2.31	1.81	104.1	−179.0	−92.9
	2.41	1.52	105.6	−179.8	52.0
	2.47	1.39	103.3	−178.9	143.3
	3.22	0.39	−86.8	−60.4	5.7
	3.84	0.14	84.6	64.9	145.5
	3.89	0.13	85.1	64.1	−91.3
	14.3		5.0	60.1	−74.9
7	0.00	96.2	93.9	−56.7	5.8
	2.05	2.20	−87.7	73.6	−84.1
	2.23	1.58	93.3	−55.9	142.9
7‡	21.8		34.8	151.3	−15.0

[a] ΔH_f: relative enthalpy of formation in kcal·mol^{-1}; ‡ = transition state, ω_1 = C_{9a}−C_9−C_{11}−C_{12}; ω_2 = C_9−C_{11}−C_{12}−C_{13}; ω_3 = C_9−C_{11}−O−H. [b] ω_2 does not exist in compound **4**. For alcohol **7**, the ω_2 values are given although they are irrelevant.

Acknowledgment. Two of us (I. de R. and M. de M.) wish to acknowledge the Comisión Interministerial de Ciencia y Tecnología (CICYT) and the Comisió Interdepartamental de Recerca i Innovació Tecnològica (CIRIT) for fellowships. Financial support was received from Direcció General de Recerca (project QFN93-4427). We thank the Servei d'Espectroscopia RMN of UAB for an allocation of spectrometer time. We thank Prof. J. Keeler for carefully reading and discussing the manuscript.

Registry numbers provided by the author: 4, 94942-50-4; **5**, 72948-52-8; **6**, 95020-55-6.

Supplementary Material Available: The aromatic region of a comparison between the simulated and the experimental spectra of the four compounds **4**−**7** and several spectra of **7** and its NOE measurements at different temperatures (7 pages). This material is contained in libraries on microfiche, immediately follows this article in the microfilm version of the journal, and can be ordered from the ACS; see any current masthead page for ordering information.